



Evaluation of quality change in *Salviae miltiorrhizae radix et rhizoma* during drying by LF-NMR and HPLC

Qinrong Liu¹ · Yishuo Wang^{1,2} · Zhenling Zhang^{1,2} · Ziwei Du¹ · Jiazhen Li¹ · Yuquan Wu¹

Received: 27 May 2021 / Accepted: 31 August 2021

© The Author(s), under exclusive licence to The Japan Society for Analytical Chemistry 2022

Abstract

Salviae miltiorrhizae radix et rhizoma (Danshen, in Chinese) is one of the traditional Chinese medicines commonly used in clinical practice. In this study, low field nuclear magnetic resonance (LF-NMR) was used to detect changes in the moisture content during the drying of Danshen. Three water states (bound, immobilized, and free) in Danshen were investigated by multi-exponential fitting of the NMR data. Mass changes during drying were analyzed using high-performance liquid chromatography and partial least squares discriminant analysis. The results revealed that two components, salvianolic acid B and tanshinone, were the main chemical substances that produced the differences. Correlations were found among chemical substances, color, and moisture. LF-NMR can quickly assess the moisture content during drying. It also provides a practical tool for the production and processing of medicines or slices.

Keywords Danshen · Low field nuclear magnetic resonance (LF-NMR) · High-performance liquid chromatography (HPLC)

Introduction

Drying is a critical processing step that promotes herbal therapeutic effects, and is an important indicator of product quality [1]. During the drying process, moisture content changes within the material cause the transformation of chemical substances that creates the unique qualities of different herbs [2]. Additionally, studies have shown that the drying conditions and moisture content affect the quality of herbal medicines [3–5]. Rhizomatic medicinal materials pose specific challenges because of their hard tissue structure, which makes them difficult to process. Over-drying or under-drying will affect the chemical composition, appearance, and performance. Rapid and nondestructive moisture

content analysis is therefore important for herbal medicine producers. Low field nuclear magnetic resonance (LF-NMR) techniques allow for the distribution and migration of components, such as water or oil in materials, to be measured from a microscopic perspective [6]. LF-NMR is an accurate and non-destructive analytical technique that has been widely used in many industries, including food production [7–9]. Studies in the field of traditional Chinese medicine (TCM) have used LF-NMR to analyze the change of the material moisture content during infiltration, rehydration, boiling, and drying [10–12]. It is also possible to classify herbs from different species or production areas using LF-NMR [13–17].

Salviae miltiorrhizae radix et rhizoma (Danshen, in Chinese) is one of the medicines commonly used in clinical practice. Danshen plays an important role in the prevention and treatment of cardiovascular diseases, and is in high demand as the main ingredient in preparations [18]. When fresh Danshen is sliced, it becomes dark brown and non-compliant within a few seconds [19]. This is explained by enzymatic changes causing the oxidation of components, but there is no specific information on which chemical components are being oxidized [20]. A previous study also found a relationship between the color change and chemical content [21]. Here, LF-NMR was used to monitor changes in

Advance Publication Released Online by J-STAGE September 10, 2021.

✉ Yishuo Wang
hnzyydx18@163.com

¹ Henan University of Chinese Medicine, Zhengzhou 450046, Henan, China

² Henan Integrated Engineering Technology Research Center of Traditional Chinese Medicine Production, Zhengzhou 450046, Henan, China

moisture content during the drying of Danshen. The color technique was used to determine the color difference characteristics of samples under different conditions and chemical composition was analyzed using high-performance liquid chromatography (HPLC).

Experimental

Sample preparation

Samples were dried at 40 °C using a constant-temperature air drying oven. Each sample was dried at an interval of four hours and measured after the temperature stabilized. Parts of the root strips at four hours intervals were cut into slices of 2–4 mm thickness for testing.

LF-NMR measurements

LF-NMR measurements were performed using an NMR Analyzer (NMI20-40H-I, Niumag Corp., Suzhou, China) equipped with a 0.5 T permanent magnet and a proton resonance frequency of 20 MHz at 32 °C. Samples were placed in an NMR tube with an aperture of 40 mm. The center frequency of the sample was obtained by the hard pulse-free induction decay sequence, and the transverse relaxation time of the sample was measured by the Carr–Purcell–Meiboom–Gill (CPMG) pulse sequence, the CPMG π -value (time between 90° pulse and 180° pulse) of 5.6 and 12.8 μ s, respectively. Transverse relaxation time (T_2) analysis and distributed exponential curve fitting were performed using MultiExp Inv Analysis software (Niumag Corp., Suzhou, China). A fitting analysis was performed on the relaxation data using a modified inversion algorithm to obtain an improved fitting. The transverse relaxation time (T_2) and its corresponding water population area ratio (A_2) were recorded. Each sample was evaluated in triplicate. Each test was measured three times to take an average.

Color analysis

The color values ΔL^* , Δa^* and Δb^* were quantified using an HP-C220 precision chromometer in the color space. The lighting source was D65 with a slit width of 1.00 nm and a field of view of 10°. ΔL^* represents the lightness with color values of from 0–100, with higher values being brighter. The Δa^* and Δb^* values went positive and negative. A positive Δa^* color value indicated red; a negative Δa^* color value indicated green. Similarly, positive values of Δb^* were yellow and negative values were blue. The sample powder was taken out and spread on the test site of the instrument, and the average value was calculated by repeating parallel scans 10 times.

High-performance liquid-phase experiment

HPLC was composed of binary LC-16 pumps (Shimadzu, Japan) and an SPD-16 UV detector (Shimadzu, Japan). Data processing was performed with LC-Solution software. The analytical column was a Hypersil GOLDC18 (4.6 × 250 mm, 5 μ m). The injection volume was 10 μ L and the detecting wavelength of the UV detector was set at 270 nm. The mobile phase was acetonitrile (A)-0.1% phosphoric acid aqueous solution (B) at the gradient program: 0–20 min, 20–26% A; 20–21 min, 26–60% A; 21–29 min, 60% A; 29–46 min, 60–65% A; 46–47 min, 65–85% A; 47–49 min, 85% A; 49–65 min, 85–20% A. The flow rate was 1.0 mL/min and the column temperature was 30 °C.

Preparation of sample solutions

The samples were crushed with a pulverizer and the particle size of the samples was 65 mesh. The powdered samples were weighed accurately. The ultrasonic treatment conditions were set to 140 W and the frequency was 42 kHz. The extraction was ultra-sonicated with 50 mL of methanol for 30 min. The sample solution was filtered through a 0.22 μ m membrane filter and analyzed by HPLC.

Preparation of standard solutions

Each standard was accurately weighed and dissolved, respectively, to get a single standard solution. A mixed standard working solution was obtained by mixing a single standard to achieve the desired concentration. All of the solutions were filtered through a 0.22 μ m membrane filter before HPLC analysis.

Results and discussion

Linear relationship between signal intensity and moisture content

During LF-NMR detection, the signal intensity of the solid material after a relaxation time of 60 μ s was taken as the total signal intensity of free water and bound water. The signal intensity could then be correlated with the water content of the standard. To verify the accuracy of the water measurements, the standard was placed in the same test conditions as the sample. The moisture content was used as the x -axis and the signal intensity was used as the y -axis when plotting results. The fitted linear equation obtained

was $y = 1678.6x + 75.522$ with a correlation coefficient of $R^2 = 0.999$, showing a significant linear relationship.

Moisture changes during drying of Danshen

First, the moisture contents of Danshen were observed at different drying times. The transverse relaxation times and peak areas were measured, and are shown in Fig. 1A. The moisture content could be quantified from the LF-NMR relative peak area results. At the beginning of drying, the moisture content in fresh roots could be divided into free, immobilized, and bound states. The peak position and area were observed to change as the drying time increased. After 16 h of drying, the amount of free water detected had decreased significantly, and became bound water. After 24 h of drying, all free water had disappeared. The results of the study indicate that the moisture content within the sample decreased continuously. An increased drying time decreased the lateral relaxation area, which implies that there was less free water inside the sample.

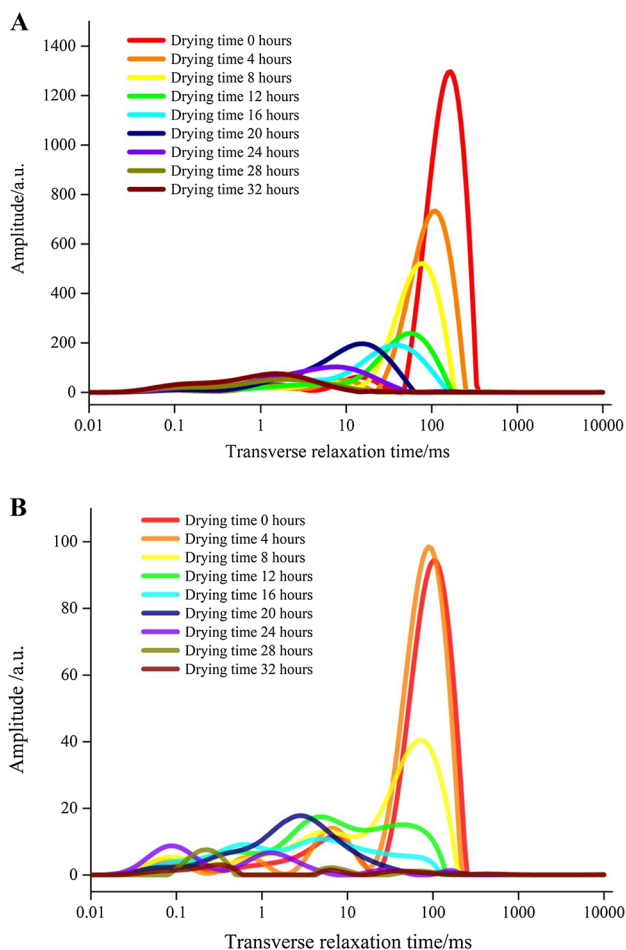


Fig. 1 Transverse relaxation time of roots (A) and slices (B) at different drying times

Drying to the desired moisture content for processing into tablets ensured the quality of any subsequent decoction [22]. Figure 1B shows the moisture content and peak area of slices at different drying times. The relaxation curves measured during the drying process showed three distinct absorption peaks. The internal bound water state of the sample was presented in the range of T_{21} , and the free water state was presented in the regions of T_{22} and T_{23} . During the drying process, the larger T_{21} indicated a higher free water content that could be easily removed. As the drying time increased, the water mobility slowed and the peak area decreased. When drying for 16 h, the sample moisture reached equilibrium. These results show that the moisture content in the slices decreased as drying time increased.

The moisture contents in roots and slices were also obtained using magnetic resonance imaging (MRI). Figure 2 shows those results: red represents high moisture content and green represents the desired moisture content. It can be concluded that the total moisture content of the fresh roots decreased significantly during drying. An increasing drying time caused significant decreases in the moisture content, with water being transported through the outer layer of the roots. The free water flowed out of the sample as the drying time increased. When drying reached 12 h, the free water decreased, as illustrated by the red part of the MRI images. After 28 h of drying, no imaging was observed. The location of the water moved from the inside to the outside during drying of the slices. The images of the sections were gradually blurred until 20 h. After this, the fibrous tissue was destroyed, and a small amount of bound water remained. After 24 h of drying, the moisture content in the internal tissues was negligible and the critical point of drying was reached, which was indicated by blurred images.

Color detection

The color difference test can be a quick and effective method to judge the quality of herbs on the basis of the magnitude of the color value. After slicing, Danshen slices showed yellow color on the cut surface, which met the standard appearance requirements. In this section, the color during the drying process was objectively displayed using the color difference value (see Fig. 3). First, roots and slices had significant differences in color changes between 16 and 24 h. Second, the results from the root showed a large variation in the color difference; Δa^* was measured with the extension of the drying time. The Δa^* maximum value was seen at 16 h of drying and the Δa^* minimum value at 24 h. Moreover, at 20 h of drying, the outer skin of the roots showed a bright red color. Correspondingly, the value of color difference, ΔL^* , decreased dramatically after 28 h, when only bound water remained in the root. Finally, a large difference in the color change was found in the section measurement results,

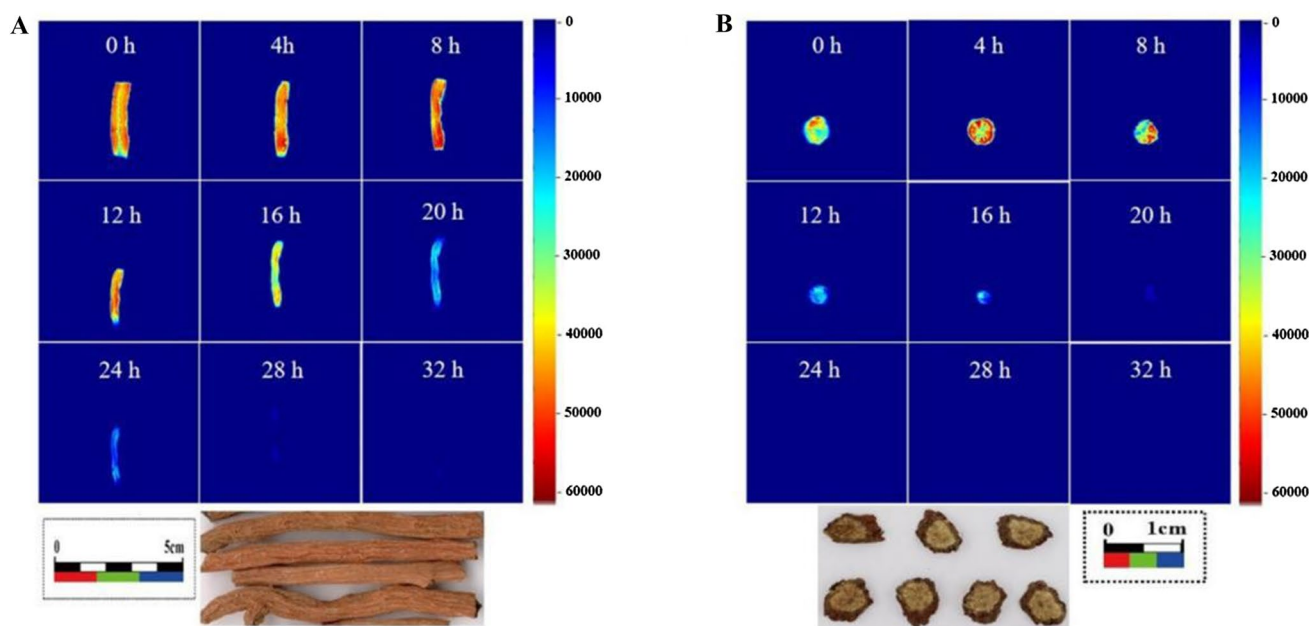


Fig. 2 MRI images of roots (**A**) and slices (**B**) at different drying times

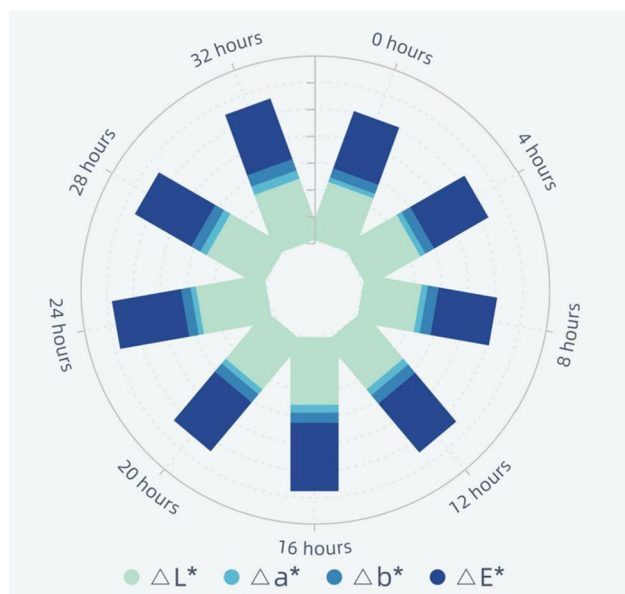


Fig. 3 Chromatic aberration value of root and slices at different drying times

and the color difference, Δa^* , appeared to decrease at 16 h of drying. However, it increased again as the drying time increased until 32 h. The value of the color difference, Δb^* , which represents the yellow color, was in excellent condition at 20 h, and met the standard appearance requirements. Similarly, the value of the color difference, ΔL^* , changed more after 24 h of drying. Therefore, according to an analysis

of the color difference test results, the color change onset begins after 20–24 h of drying.

Changes in chemical composition during drying

Identification of chromatography peaks

The fingerprint of samples was established using HPLC. Figure 4A shows a chromatogram of the standards and samples. Fifteen common peaks were collected with satisfactory peak signals and reasonable resolutions in each batch of sample, where the appearance ratio of the total common peak was 90%. Eight of the common peaks were identified by matching the retention time to the respective reference compounds. Peaks 2, 4, 5, 6, 9, 11, 12 and 14 were danshensu (DSS), rosmarinic acid (RA), lithospermic acid (LA), salvianolic acid B (SAB), dihydrotanshinone (DDT), cryptotanshinone (CT), tanshinone I (T I) and tanshinone IIA (T IIA), respectively.

Method validation of HPLC fingerprint analysis

The analytical method of HPLC fingerprint analysis was validated for precision, reproducibility, and stability. Peak 6 was chosen as a reference substance (SAB) to calculate the relative retention times (RRTs) and the relative peak areas (RPAs) in all samples. Table 1 shows the precision, reproducibility, and stability tests; the relative standard deviations (RSD) of RRTs were in the range of 0.08–1.04%, 0.07–1.36%, and 0.08–1.58%, the RSDs of RPAs were in

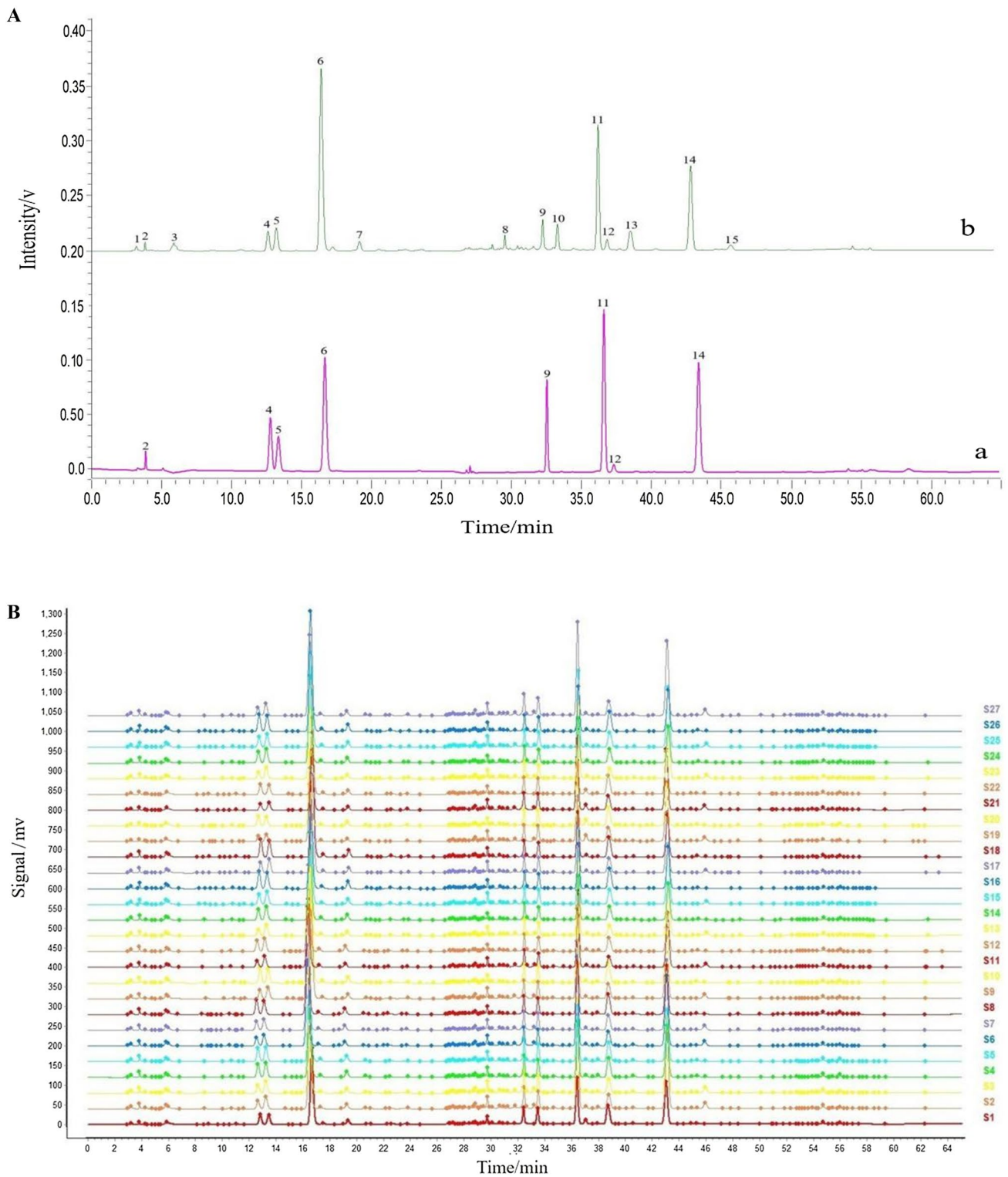


Fig. 4 Chromatogram (**A**) and fingerprint information (**B**). **A** 2. Danshensu; 4. rosmarinic acid; 5. Lithospermic acid; 6. Salvianolic acid B; 9. Dihydrotanshinone; 11. Cryptotanshinone; 12. Tanshinone I; 14. Tanshinone II_A; S1, Samples; S2, Standards. **B** S1–S3, drying

time 0 h; S4–S6, drying time 4 h; S7–S9, drying time 8 h; S10–S12, drying time 12 h; S13–S15, drying time 16 h; S16–S18, drying time 20 h; S19–S21, drying time 24 h; S22–S24, drying time 28 h; S25–S27, drying time 32 h

Table 1 Analytical results of precision, stability, and reproducibility tests for RRTs and RPAs of fifteen characteristic common

No.	RSD of RRTs, %			RSD of RPAs, %		
	Precision	Stability	Reproducibility	Precision	Stability	Reproducibility
1	0.08	0.79	0.08	0.53	0.69	2.52
2	0.15	0.77	0.21	0.94	1.20	2.51
3	1.40	0.96	0.94	1.40	2.13	1.88
4	0.87	1.40	1.05	1.25	2.86	1.85
5	1.04	1.60	1.31	2.71	2.57	2.17
6	0.78	1.36	0.96	1.14	2.47	2.55
7	0.58	1.23	0.65	1.82	2.12	2.48
8	0.04	0.07	1.58	1.11	1.39	1.90
9	0.06	0.16	0.03	2.12	2.20	2.93
10	0.07	0.18	0.03	2.50	1.16	0.69
11	0.09	0.24	0.03	0.90	2.42	1.30
12	0.10	0.27	0.05	2.98	1.69	1.73
13	0.10	0.27	0.03	1.46	2.40	1.92
14	0.11	0.38	0.02	1.41	2.60	2.28
15	0.12	0.43	0.02	1.89	2.92	1.55

the range of 0.53–2.98%, 0.69–2.92%, and 0.69–2.93%, respectively.

Similarity evaluation

Similarity is an important parameter of the HPLC fingerprint [23]. The original HPLC data were input to the system to determine the similarity, which was used to characterize the sample. The similarity results were calculated using the software of “Similarity Evaluation System for Chromatographic Fingerprint of TCM (2012A)”. Chromatograms of Danshen samples that were dried for 0 h were identified as reference controls. In Fig. 4B, the effect of the drying time on the sample is fully evaluated. The sample similarity value was greater than 0.90, which indicates that the roots and slices with different drying times had stability and consistency. Thus, the chemicals contained in medicines did not change during the drying process, but the relative composition did.

Validation of quantitative methods

The method of quantitative analysis was validated using the linearity, precision, stability, repeatability, and recovery tests. Mixed control solutions with known mass concentrations were prepared according to the standard solution operation method. The components used to prepare the control solutions were DSS, RA, LA, SAB, DDT, CT, T I, T II_A. Table 2 showed all compounds have good linearity ($R^2 > 0.9$) over the tested ranges. The precision of the instrument was determined by analyzing standard solutions; the results show that the precision was within the required range. The stability of these eight compounds was tested at 0, 4, 8, 12, 24, and 48 h, and all compounds were found to be stable over the testing period. The recovery was validated using a standard spiking test. The result showed that the average recovery values for the marker compounds were between 9 and 10%, where the RSD was 1–2%, which suggests that the method was precise and accurate.

Table 2 Calibration curve, precision, stability, repeatability and recovery results of eight chemical components

Compound	Standard curve	R^2	Linear range/ $\mu\text{g mL}^{-1}$	Precision (RSD), %	Stability (RSD), %	Repeatability (RSD), %	Recovery, %
DSS	$Y = 1,590,615.3106X + 2206.4286$	0.999	4.976–59.712	2.16	2.33	2.51	99.60
RA	$Y = 10,432,334.8516X - 1531.8571$	0.999	4.575–54.900	1.18	0.94	0.79	101.30
LA	$Y = 9,354,963.7955X - 2160.2143$	0.999	4.086–49.032	0.94	0.88	1.44	99.48
SAB	$Y = 5,747,761.8763X + 2809.1429$	0.999	20.900–250.800	1.32	1.13	0.99	102.18
DDT	$Y = 25,097,229.8440X - 46.3571$	0.999	2.890–34.680	2.68	2.75	2.42	100.57
CT	$Y = 75,989,668.7877X + 3599.8571$	0.999	4.005–48.060	1.14	1.15	1.38	100.05
T I	$Y = 4,230,873.3787X - 12,955.7143$	0.996	6.344–76.128	2.84	2.38	2.52	96.21
T II _A	$Y = 63,794,121.8454X + 2984.5714$	0.999	3.750–45.000	1.11	0.79	0.83	102.33

Quantitation of constituents

HPLC is indispensable in various analytical fields [24]. The effect of the drying time on the composition of Danshen was evaluated using HPLC; the results are shown in Fig. 5. Initially, the content of phenolic acid components was relatively low, but this doubled by the end of the drying time. The content of the tanshinone components showed an irregular trend, reaching its highest value at between 16 and 20 h of drying. After different drying times, the samples were compared with fresh herbs. SAB, DDT and CT had significant differences at 4 h of drying. At 12 h of drying, DSS showed a difference. At 16 h of drying, all eight chemical components showed significant differences. The experimental results indicate that the drying time affects the chemical composition of Danshen. On the basis of these results and those of the color difference experiment, we concluded that the color of Danshen obtained after drying for 20 h satisfied the standard requirements. LF-NMR showed strong changes in the moisture distribution at between 20 and 24 h of drying, and the moisture content after this is suitable for further applications [23]. A significant positive correlation was also found between the dehydration rate and the content of the phenolic acid components. Ultimately, these results show that controlling the drying time is important.

Multivariate analysis

Principal component analysis (PCA) is an unsupervised classification pattern recognition method with is used for data compression and dimension removal [25]. With the

PCA, those samples with different drying times were separated clearly (see Fig. 6A). The results showed that samples were better separated between the groups, indicating the difference between the groups. A partial least squares discriminant analysis (PLS-DA) can be used to screen out changes in data that are independent of independent and categorical variables [26]. In Fig. 6B, PLS-DA was used to analyze the chemical constituents of root strips with different drying times. In Fig. 6B, the early stage of drying (0–12 h) was a group. The drying phase was then divided into two groups (16–20 h and 24–28 h). Finally, the end of drying (32 h) was also categorized as a group.

The technique maximizes the separation of pre-defined and classified information in the matrix [27]. Moreover, tests were performed with established PLS-DA models to assess the validity of the results. In Fig. 6C, the permutation test model R^2X , R^2Y , and Q^2 values are 0.9, 0.8, and 0.6, respectively. The R^2 , and Q^2 values were higher in the models than in the permuted ones, and the regression line of the permuted Q^2 -points intersected the vertical axis. These results indicate high suitability and predictiveness of the developed model. Additionally, the contribution of the compounds to the sample identification was calculated and the variables of variation were ranked. Figure 6D shows that the factors affecting the difference in the quality of Danshen with different drying times could be two chemical components, SAB and tanshinone.

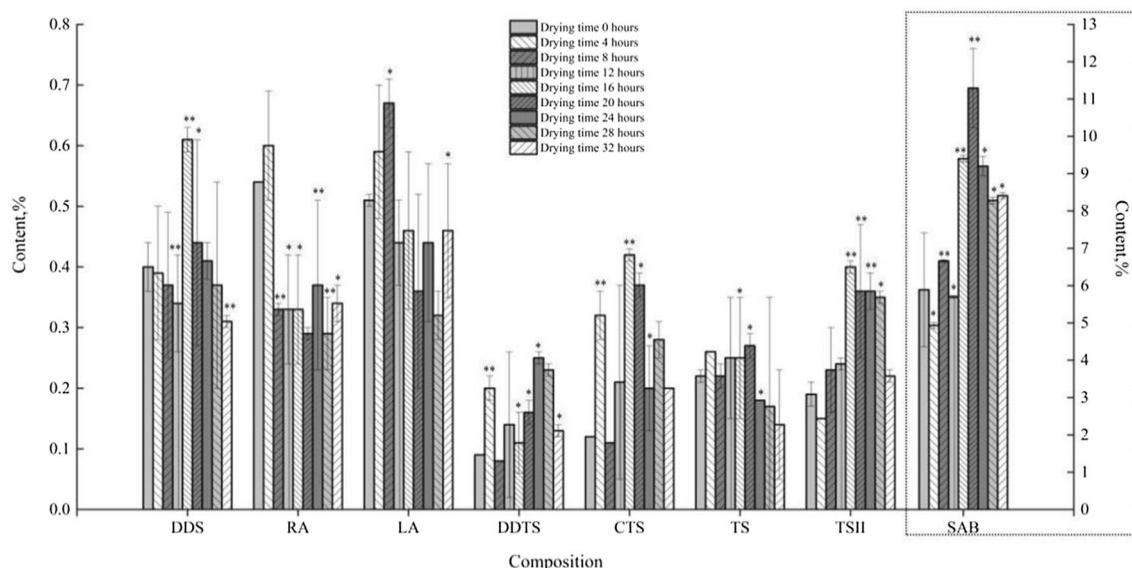


Fig. 5 Changes in the content of chemical components at different drying times. ** $P < 0.01$, significant at the 0.01 level, compared with the dry time, 0 h. * $P < 0.05$, significant at the 0.05 level, compared with the dry time, 0 h

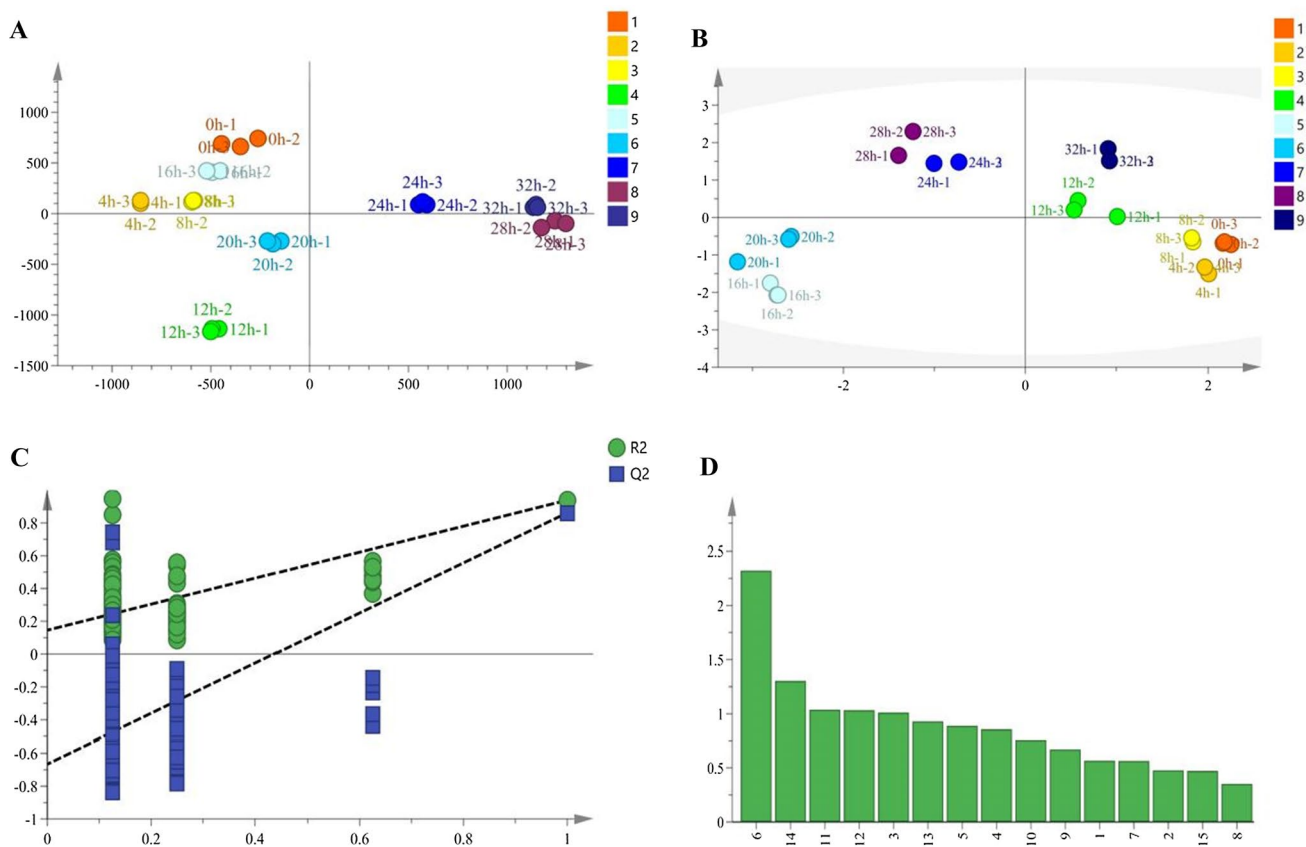


Fig. 6 PLS-DA score plot (A), permutation test model (B), PCA (C), and VIP value (D). A and C 1, drying time, 0 h; 2, drying time, 4 h; 3, drying time, 8 h; 4, drying time, 12 h; 5, drying time, 16 h; 6, drying time, 20 h; 7, drying time, 24 h; 8, drying time, 28 h; 9, drying time, 32 h

Correlation analysis

As a fast and non-destructive analytical technique, LF-NMR can replace other time-consuming methods if the relationships between the LF-NMR parameters and the relative physio-chemical parameters can be determined [28]. The relationships among moisture content and LF-NMR parameters were investigated. Table 3 shows significant correlations with A_{21} and Δa^* , with coefficients of 0.784 and 0.885, respectively. There were also significant correlations with T_{21} , T_{22} , and A_{21} ,

with coefficients of 0.964, 0.958, and 0.875, respectively. The color value showed significant correlations with A_{23} and Δa^* , with coefficient of 0.693, respectively. Meanwhile, there was a relationship between the moisture content and the color, which was consistent with previous experimental studies [29]. The color difference experiment found that the root appearance and color of the samples obtained at 20 h of drying met the standard requirements. Some studies showed that processing at this moisture content is very suitable. This indicates that the color characteristics of “skin” are more important than “flesh”

Table 3 Correlation coefficient among MC, area and color parameters

	MC	A_{21}/g	A_{22}/g	A_{23}/g	ΔL^*	Δa^*	Δb^*
MC	1.000	0.784*	0.014	0.666	0.527	-0.885**	-0.416
A_{21}/g		1.000	-0.434	-0.341	-0.407	0.650	0.208
A_{22}/g			1.000	-0.090	0.157	-0.090	-0.078
A_{23}/g				1.000	0.441	-0.693*	-0.466
ΔL^*					1.000	-0.824**	-0.859**
Δa^*						1.000	0.777*
Δb^*							1.000

* $P < 0.05$, significant at the 0.05 level

** $P < 0.01$, significant at the 0.01 level

Table 4 Correlation coefficient among composition content and color parameters

	DSS	RA	LA	SAB	DDT	CT	T I	T II _A	ΔL^*	Δa^*	Δb^*
DSS	1.000	-0.286	0.215	-0.866**	-0.342	0.426	0.461	-0.033	-0.212	-0.674*	-0.291
RA		1.000	-0.481	0.208	0.550	0.300	-0.100	0.332	0.617	0.361	-0.348
LA			1.000	-0.324	-0.182	-0.449	-0.069	-0.637	-0.513	-0.571	0.052
SAB				1.000	-0.041	-0.136	-0.470	0.048	0.125	0.877**	0.619
DDT					1.000	-0.269	-0.149	0.085	0.361	0.006	-0.465
CT						1.000	0.658	0.550	0.508	0.074	-0.176
T I							1.000	0.598	0.489	-0.407	-0.526
T II _A								1.000	0.728*	0.320	-0.259
ΔL^*									1.000	0.305	-0.339
Δa^*										1.000	0.631
Δb^*											1.000

* $P < 0.05$, significant at the 0.05 level

** $P < 0.01$, significant at the 0.01 level

in the traditional evaluation method of “skin, red, flesh, and purple,” and the color difference of skin is related to the quality difference of the herbs.

To verify whether the chemical substance changes during drying were correlated with color, the correlation between the color difference values and the chemical composition content was further analyzed. The correlation between the color difference values of the samples obtained at different drying times and the corresponding chemical composition were analyzed separately. Table 4 shows that there was significant correlation between Δa^* and component DSS, with a correlation coefficient of 0.886. Similarly, component SAB also showed a significant positive correlation with Δa^* , with a correlation coefficient of 0.877. Component T II_A showed a correlation with ΔL^* , with a correlation coefficient of 0.728. Therefore, and given the correlation between the moisture content and color, we speculated that there was a correlation with the decrease of the moisture content and a gradual increase of the phenolic acid components caused by drying. Some experiments found that Danshen had accumulated a large amount of bound phenolic acid components during the growth process, and that the free phenolic acid, such as component SAB, was dissociated by bound phenolic acid under the action of related enzymes during the drying process [21]. Our results show that when the drying time was 16–20 h, the component SAB content was at its highest. Moreover, at this drying time, the moisture content and the color difference values met the required standards.

Conclusion

The drying time affects the chemical composition and color change of Danshen. LF-NMR can quickly and accurately detect changes of the moisture content inside medicines,

which provides a convenient and efficient detection tool for moisture control during the processing of herbal medicines. This suggests that own technique can be used with processing applications of TCM. A correlation was found between the process drying time and the moisture content, chemical composition, and color. Meanwhile, as the moisture content of the samples decreased, the phenolic acid components and single similar components changed significantly, and differences in the color were produced. We speculate that salvianolic acid and tanshinone might be the main chemical components that produced the differences.

Acknowledgements This work was financially supported by China National Administration of TCM Public Welfare Industry Special Project (00104296), and the Science and Technology Innovation Project of Henan Province (184100510017). We thank Shaun Galbraith, PhD, from Liwen Bianji (Edanz) (<http://www.liwenbianji.cn/>) for editing the English text of a draft of this manuscript.

Declarations

Conflict of interest The authors declare no conflict of interest.

References

1. C. Yao, X.D. Qian, G.F. Zhou, S.W. Zhang, L.Q. Li, Q.S. Guo, *Food Sci. Biotechnol.* **28**, 355 (2019)
2. X.S. Liu, Z.F. Qiu, L.H. Wang, Y. Chen, *Food BioProd. Process.* **89**, 10 (2011)
3. C.K. Bai, J.J. Yang, B. Cao, Y. Xue, P.F. Gao, H. Liang, G.S. Li, *Ind. Crops Prod.* **158**, 112985 (2020)
4. S. Rafiq, B. Singh, Y. Gat, *J. Food Sci. Technol.* **56**, 2458 (2019)
5. W.W. Kuang, Z.F. Wu, N. Wan, Y.H. Li, X.C. Wang, C.C. Kang, Z.F. Liu, M. Yang, *Chin. Tradit. Herb. Drugs* **44**(15), 3195 (2019)
6. X.L. Shao, Y.F. Li, *Food Bioprocess Technol.* **5**, 1817 (2012)
7. S.Y. Lin, S.L. Yang, X.F. Li, F. Chen, M.D. Zhang, *Food Chem.* **199**, 280 (2016)

8. M.Q. Tan, Z.Y. Lin, Y.X. Zu, B.W. Zhu, S.S. Cheng, *Food Res. Int.* **109**, 65 (2018)
9. X.L. Zhou, Y. Chen, Q. Yang, Y.N. Liu, Y.C. Wu, R.S. Lu, Z.H. Ni, *Anal. Sci.* **35**, 1381 (2019)
10. P. Berman, A. Leshem, O. Etziony, O. Levi, Y. Parmet, *Biotechnol. Biofuels* **6**, 55 (2013)
11. F.F. Xu, X. Jin, L. Zhang, X.D. Chen, *Food Res. Int.* **96**, 191 (2017)
12. Cui. Li, Y.N. Chen, M. Li, T.Y. Liu, P. Yang, L.P. Guo, X. Wang, *Dry. Technol.* **38**, 304–312 (2020)
13. Q.S. Liu, Y. He, Q.F. Cao, S.Z. Xu, X.Y. Rao, X.J. Luo, *China J. Chin. Mater. Med.* **45**(20), 4882 (2020)
14. Y. Zheng, L. Lei, J. Ai, S. Liang, X. Deng, L. Shi, Z.N. Mei, Y.S. Ren, *Chin. Tradit. Herb. Drugs* **50**(14), 3302 (2019)
15. W.J. Duan, Y. Li, L. Cui, F. Liu, G.H. Yang, L.P. Guo, X. Wang, *China J. Chin. Mater. Med.* **42**(11), 2092 (2017)
16. Y.N. Chen, H.J. Dong, J.K. Li, L.P. Guo, X. Wang, *Molecules* **24**, 2 (2019)
17. L.L. Li, M. Zhang, P.Q. Yang, *Lebensm. Wiss. Technol.* **105**, 257 (2019)
18. Z.Q. Jiang, W. Gao, L.Q. Huang, *Front. Pharmacol.* **10**, 202 (2019)
19. X. Chen, Z.F. Huang, Y. Chen, Y.H. Liu, J.H. Yi, *China J. Chin. Mater. Med.* **46**(05), 1145 (2021)
20. X. Zhang, X.Q. Li, Y. Wang, L.Y. Li, Y.J. Dai, Q.H. Wang, *Chin. Tradit. Herb. Drugs* **49**(17), 4029 (2018)
21. T. Zhou, C.M. Luo, S.L. Zhang, Z.F. Huang, Y.N. Tang, Y.H. Liu, Y. Chen, Q.M. Li, J.H. Yi, *China J. Chin. Mater. Med.* **44**(21), 4634 (2019)
22. Z.G. Zhao, X.R. Gao, B.B. Yan, J. Xie, X.M. Zhang, J. Li, J.L. Hou, W.Q. Wang, *China J. Tradit. Chin. Med. Pharm.* **32**(02), 797 (2017)
23. F.F. Yang, T.T. Chu, Y.J. Zhang, X.T. Liu, G.X. Sun, Z.H. Chen, *Food Chem.* **324**, 126854 (2020)
24. S. Kitagawa, *Anal. Sci.* **35**, 949 (2019)
25. X.X. Liu, H. Wang, X.Y. Huang, M. Guo, Z.G. Yang, K.X. Zhang, J.F. Liu, M.H. Wang, Y. Gong, J.T. Wei, D.L. Di, *Food Anal. Methods* **13**, 2222 (2020)
26. Q. Peng, X. Xu, W.H. Xing, B.W. Hu, C. Shen, R.G. Tian, X.M. Li, Q.X. Xu, J.Y. Chen, F.R. Chen, H.J. Zou, G.F. Xie, *Innov. Food Sci. Emerg. Technol.* **44**, 212 (2017)
27. S. Kasemsumran, N. Suttijitpukdee, V. Keeratinijakal, *Anal. Sci.* **33**, 111 (2017)
28. Y. Chen, M. Li, T.S.K. Dharmasiri, X. Song, F. Liu, X. Wang, *Food Chem.* **306**, 125625 (2020)
29. Q.R. Liu, Y.S. Wang, Z.L. Zhang, Y.B. Shi, Z.Y. Lin, *Nat. Prod. Res. Dev.* **33**(05), 802 (2021)